Application of the projected Hartree-Fock method to rotational motion in $1p$-shell odd-A nuclei

F. Brut and S. Jang

Institut des Sciences Nucléaires, BP 257, 38044 Grenoble-Cédex, France

(Received 4 March 1976)

The rotational properties of $A = 7$, 9, 11, and 13 nuclei are studied in a self-consistent way using the effective two-body interactions derived either from the Sussex relative harmonic-oscillator matrix elements or from energy-level fitting. Special care is taken in choosing the appropriate solution among others corresponding to oblate or prolate deformed orbitals. In particular, a pronounced band mixing in $A = 9$ and $A = 11$ nuclei is investigated by diagonalizing the effective Hamiltonian within the orthonormalized basis setup with the Hartree-Fock projected states. Moments of inerita of $A = 6$, 8, 10, and 12 nuclei are also computed by means of the cranking model. The energy levels and the magnetic dipole moments, as well as the $M1$ transition rates, are in good agreement with shell-model calculations which use the same effective two-body interactions.

NUCLEAR STRUCTURE ^{7}Li, ^{9}Be, ^{11}B, ^{13}N; calculated levels, moments, and transition rates. Calculated moments of inertia of $A = 6$, 8, 10, and 12 nuclei. Projected Hartree-Fock method, cranking model.

I. INTRODUCTION

Several authors[1] have attempted to interpret the low-lying energy levels of $1p$-shell nuclei within the framework of the strong coupling rotational model. The applicability of the unified model in this region is based on the fact[2] that there exists a strong overlap between the groups of low-lying states obtained by intermediate coupling and the generating procedure based on the Nilsson's deformed potential. Thus collective models have had some success in fitting experimental energy levels, but they often fail when checked with other observables, such as ground state binding energies, electromagnetic transition rates, and particle scattering. In particular, application of the macroscopic rotational model to the $1p$-shell nuclei sometimes requires the introduction of some phenomenological parameters without consideration of their physical significance.

It is known that Hartree-Fock intrinsic states generate rotational bands in deformed nuclei.[3] Kelson and Levinson[4] performed single major-shell Hartree-Fock (HF) calculations and studied rotational band mixing of odd-A sd-shell nuclei in a self-consistent but adiabatic way in the sense that they diagonalized the rotation-particle coupling interaction. The HF theory has since been extended to multishell calculations and thus the projected HF[5] calculations have become more frequent. Bassichis, Giraud, and Ripka[6] have shown that the HF theory together with the angular momentum projection is a useful approximation to the configuration-mixing calculations. There exists a number of projected HF calculations for finite nuclei,[7] mostly on the sd shell, but the problem of rota-

tional band mixing for $1p$-shell nuclei has not yet been investigated in a self-consistent way. It is thus felt that too little attention has been given in the past to the possibility of using a shell-model Hamiltonian in calculation of collective properties of very light odd-A nuclei, and in particular in calculation of the rotational band mixing.

The aim of this work is therefore to fill a gap in this field of inquiry by studying nuclear collective properties of $1p$-shell nuclei in a self-consistent way. It was also considered useful to compare the projected HF calculations with an exact diagonalization in a few cases of very light nuclei.

Because of their relative simplicity, the $1p$-shell nuclei have been studied in considerable detail by means of exact shell-model calculations using different kinds of effective two-body potentials,[8-10] mostly derived from realistic nucleon-nucleon (NN) interactions. The validity of using such effective two-body forces in the HF theory has been discussed by many authors.[11] However, for multishell HF calculations the search for a suitable potential applicable throughout all major shells appears to be more difficult. For example, Gunye, Law, and Bhaduri[7] have shown that the effective forces derived from the NN Yale potentials and from the NN phase shifts drastically underbind the nuclei of mass $A = 7$, 8, and 9. They were able to reproduce the experimental binding energies by arbitrarily increasing the $^3S_1$ matrix elements in the both forces but failed to obtain reasonable values of the rms radii.

Owing to the difficulty of choosing an appropriate realistic two-body interaction for projected multishell HF calculation and, in particular, in view of

the fact that the object of the present study is to investigate the collective features of the low-lying normal parity states in connection with shell-model calculations, we use effective two-nucleon interactions taken from shell-model studies without further discussing their validity. Because of this choice of effective interaction, we restrict ourselves to the single major-shell HF calculation and the comparison between projected HF formalism and shell-model calculation is thus relatively easy to visualize. Although the HF wave functions obtained in this manner are not stable against particle-hole excitations, and such calculations at best minimize the potential energy, it is highly possible that the main features of the collective properties of the low-lying normal parity states of odd-A p-shell nuclei are governed by nucleons in the p-shell orbits.

We therefore have performed calculations for $A = 7$, 9, 11, and 13 nuclei using alternatively the effective two-body interaction of Hauge and Maripuu,[9] derived from the Sussex relative harmonic oscillator matrix elements, and that of Cohen and Kurath,[8] designated as (6–16) two-body matrix elements (2BME), derived from energy-level fitting. In Sec. II we discuss briefly how the HF intrinsic states generate rotational bands in deformed nuclei and present the method used for the band-mixing calculations. This section contains also details of the actual HF computation connected with the effective two-body interactions and with the effect of the center of mass correction. In Sec. III, spectra, magnetic moments, and $M1$ transitions, as well as moments of inertia obtained by means of the cranking model, are described and presented with the help of tables and figures. These results are compared with those obtained from the shell-model calculations of Cohen and Kurath[8] (to be referred as SM-I) and of Hauge and Maripuu[9] (to be referred as SM-II). The conclusions are presented in Sec. IV.

II. METHOD OF CALCULATION

The HF method of solving for self-consistent single-particle wave functions and energies is that of Ripka[3] and Kelson.[4] Following Ripka, an inert core of ^{16}O is assumed and intrinsic deformed orbitals in an axially symmetric field are built for $1p$-shell nucleons which occupy the $1p_{3/2}$ and $1p_{1/2}$ hole subshells. It is also assumed that there exist no dominant pairing effects which lead to a breakdown of the validity of single determinant wave functions.

The HF Hamiltonian matrix which takes account of the center of mass correction has the form

$$\langle jm\tau | h | j'm'\tau \rangle = \langle h_0 \rangle + \sum_{\mu=1}^{N_p} \langle jm\tau, \mu | v' | j'm'\tau, \mu \rangle - \sum_{\nu=1}^{N_h} \langle jm\tau, \nu | v' | j'm'\tau, \nu \rangle, \tag{1}$$

where N_p and N_h denote, respectively, the number of particle and hole orbits. The $\langle h_0 \rangle$ represents the HF Hamiltonian of the closed shell solution of ^{16}O and has the form

$$\langle h_0 \rangle = \frac{A-1}{A} \langle jm | t | j'm' \rangle + \sum_{\lambda \in 1s, 1p} \langle jm\tau, \lambda | v' | j'm'\tau, \lambda \rangle. \tag{2}$$

The HF Hamiltonian (2) is actually replaced with the single-particle energies of the ^{16}O field. The t is the kinetic energy operator and the v' is composed of two parts, the two-nucleon interaction potential v_{12} and the correction term for the center of mass motion

$$v' = v_{12} - \frac{\vec{p}_1 \cdot \vec{p}_2}{MA}, \tag{3}$$

where $\vec{p}$ is the linear momentum and M is the nucleon mass. It is now seen that the term $\vec{p}_1 \cdot \vec{p}_2$ does not contribute to the two-particle matrix elements in Eq. (1) when N_p or N_h is limited to a single major shell. It is therefore hoped that use of experimentally extracted values of single-particle energies for the HF Hamiltonian of the closed shell solution counterbalances some of the missing terms in the interaction as well as the effect of the center of mass correction in $\langle h_0 \rangle$. The situation is somewhat analogous to that in shell-model studies using a harmonic oscillator basis. Indeed, there are no spurious states arising from the center of mass motion for the states of the shell model in which there is only one shell incompletely filled and any number of other filled shells without holes.

Actually, most of the effective two-body matrix elements in the literature have been computed in connection with some fixed values of the single-particle energies or with variation of the single-particle splitting between the $p_{3/2}$ and $p_{1/2}$ nucleons. Thus, use of the effective p-shell two-body interaction does not allow us to take proper account of the effect of the center of mass correction. However, as shown in the Appendix, in which this problem is briefly discussed within the framework of multishell HF calculations, nuclear properties such as rms radii and mass-quadrupole moments of $1p$-shell nuclei are little changed by this effect. In fact, only the HF energies are affected by the center of mass correction.

Because we use here the ^{16}O core as a reference nucleus and most effective two-body interactions are derived assuming the $(1s)^4$ core as a reference, it is necessary to compute the j-dependent single-particle energies of the ^{16}O field from the corresponding single-particle energies referred to the ^{4}He core. This can be done by relating the HF Hamiltonian matrix of hole orbits to that of the particle orbits through

$$\langle jm\tau | h | j'm'\tau \rangle$$

$$= \epsilon_j^0 \delta_{jj'} \delta_{mm'} - \sum_{\nu=1}^{N_h} \langle jm\tau, \nu | v_{12} | j'm'\tau, \nu \rangle$$

$$= \epsilon_j^\alpha \delta_{jj'} \delta_{mm'} + \sum_{\mu=1}^{M_p} \langle jm\tau, \mu | v_{12} | j'm'\tau, \mu \rangle, \quad (4)$$

where M_p stands for the number of $1p$-shell particle orbits referred to the ^{4}He core. Here ϵ_j^0 refers to the single-particle energy of the ^{16}O field and

ϵ_j^α to that of the ^{4}He field. This formula is used as a method of extrapolation for obtaining ϵ_j^0 from ϵ_j^α and vice versa. Special care is taken in computation of the HF solutions, since various minima may be obtained. The HF energy minima also depend on how the occupied orbits are filled. In particular, most of the $1p$-shell nuclei have at least two different solutions corresponding to oblate or prolate deformations. It is thus important to select the solution corresponding to the lowest minimum. The ambiguity in choosing an appropriate orbital can, in principle, be removed by noting that the orbital corresponding to the lowest minimum should generate the low-lying states.

The method of angular momentum projection used is the one developed by Levinson and Unna.[12] The projected many-hole wave function of n neutrons and m protons can be expressed in terms of the product of deformed single-hole orbitals as

$$\psi_{JK} = P_M^J [\alpha_{k_1}(1) \cdots \alpha_{k_n}(n) \alpha_{k_{n+1}}(n+1) \cdots \alpha_{k_{n+m}}(n+m)] | {}^{16}O \rangle$$

$$= \sum_{J_1 M_1 J_2 M_2} \langle J_1 K_1 J_2 K_2 | JK \rangle \langle J_1 M_1 J_2 M_2 | JM \rangle \, P_{M_1}^{J_1}[\alpha_{k_1}(1) \cdots \alpha_{k_n}(n)] P_{M_2}^{J_2}[\alpha_{k_{n+1}}(n+1) \cdots \alpha_{k_{n+m}}(n+m)] | {}^{16}O \rangle, \quad (5)$$

where

$$K_1 = \sum_{i=1}^{n} k_i, \quad K_2 = \sum_{i=n+1}^{n+m} k_i,$$

and the α_k are the intrinsic deformed hole creation operators related to the operators of a spherical field by

$$\alpha_k^\dagger = \sum_j x_{jk} a_{jk=m}^\dagger, \quad (6)$$

with

$$x_{j-k} = (-1)^{j+l-1/2} x_{jk}. \quad (7)$$

The notation P_M^J stands for the many-particle projection operator defined in Ref. 12.

Finally, the projected states of a particular HF orbit are identified with the levels of a rotational band. In the case of a band-mixing calculation an orthonormal basis of projected states is set up and the nuclear Hamiltonian is then diagonalized within this basis. In the case of two-band mixing, the mixed state Ψ_{JM}, having energy E_J, can be expressed in terms of two orthonormal bases Φ_{JMK_1} and Φ_{JMK_2} as

$$\Psi_{JM} = a_{JK_1} \Phi_{JMK_1} + a_{JK_2} \Phi_{JMK_2}, \quad (8)$$

with

$$H\Phi_{JMK_i} = E_i \Phi_{JMK_i}, \quad i = 1, 2.$$

Using overlap integrals between the projected states $N_{ij} = \langle \psi_{JK_i} | \psi_{JK_j} \rangle$ and the nuclear Hamiltonian matrix $H_{ij} = \langle \psi_{JK_i} | H | \psi_{JK_j} \rangle$, the E_J and the coefficients a_{JK_2} can be written as

$$E_J = \frac{X \pm Y}{2(N_{11}N_{22} - N_{12}^2)}, \quad (9)$$

$$a_{JK_2}^2 = \frac{1}{Y} \left(N_{11}N_{22} - N_{12}^2 \right) \left(E_J - \frac{H_{12}}{N_{11}} \right), \quad (10)$$

with

$$X = N_{22}H_{11} + N_{11}H_{22} - 2N_{12}H_{12},$$

$$Y = [(N_{22}H_{11} - N_{11}H_{22})^2 + 4(N_{12}H_{11} - N_{11}H_{12})$$

$$\times (N_{12}H_{22} - N_{22}H_{12})]^{1/2}.$$

The energy E_J can also be expressed in the more familiar form

$$2E_J = E_1 + E_2 \pm [(E_1 - E_2)^2 + 4E_{12}^2]^{1/2}. \quad (11)$$

The term E_{12}^2, which corresponds to the so-called rotation-particle coupling[13] term, has the form

$$E_{12} = \frac{-N_{12}H_{11} + N_{11}H_{12}}{N_{11}(N_{11}N_{22} - N_{12}^2)^{1/2}}. \quad (12)$$

In the case of the usual rotation-particle coupling one can treat the mixing problem as a perturbation, provided that the energy of two configurations (K_1 and $K_2 = K_1 + 1$) are very different from each other so that the energy difference is larger

than the interaction energy of these configurations. In the same spirit, one may argue that the condition $E_{12}{}^2/(E_1 - E_2) \ll 1$ makes it possible to expand the square root term so as to estimate the mixing effect on the original unperturbed rotational energies.

III. RESULTS

A. Energy levels

When use is made of Eq. (4) introducing the effective matrix elements of Cohen and Kurath,[8] their single-particle energies $\epsilon_{p1/2}^\alpha = 2.27$ MeV and $\epsilon_{p3/2}^\alpha = 1.63$ MeV, referred to the ^{4}He core, yield $\epsilon_{p1/2}^0 = -16.13$ MeV and $\epsilon_{p3/2}^0 = -23.1675$ MeV, referred to the ^{16}O. The resulting splitting is 7.04 MeV, which is comparable with the experimental value 6.16 MeV. Other examples of extrapolation of the single-particle energies related to the Sussex realistic effective two-body interactions[9] are shown in Table I. In contrast to the constant energy splitting in the first example, the fluctuation of the splitting in Table I is rather important. It is noted that the approximately constant value of splitting at around 7 MeV for $A \geqslant 10$ nuclei corresponds to about 9 MeV with respect to the ^{16}O field.

As was discussed in the previous section, improperly chosen orbitals having an inappropriate deformation often lead to binding energies far from the expected values. Thus the oblate solutions are generated for the nuclei of mass 11 and 13, whereas the prolate solutions are taken for the nuclei of mass 7 and 9. Table II shows the resulting binding energies of the ground states, compared with the shell-model calculation of SM-I. Experimental nuclear binding energies are also indicated. The agreement between the two calculations is fairly good. Figures 1 through 4 show the resulting spectra of ^{7}Li, ^{9}Be, ^{11}B, and ^{13}N calculated with both of the effective two-body interactions we have discussed. These spectra are compared with the shell model calculations of SM-I and SM-II. The over-all comparison indicates

TABLE I. Single-particle energy splittings $\Delta\epsilon = \epsilon_{p1/2} - \epsilon_{p3/2}$, required for use of the realistic Sussex interactions. Row 1 lists the calculated splittings which are referenced to the ^{16}O core, and row 2 shows the corresponding splitting in the field of ^{4}He.

Single-particle energy splitting	^{7}Be	^{9}Be	^{11}B	^{13}C
$\Delta\epsilon(^{16}$O) (MeV)	7.2	5.4	9.3	9.8
$\Delta\epsilon(^4$He) (MeV)	3.4	2.8	6.7	7.2

TABLE II. Nuclear binding energies for the ground states. To facilitate comparison all values are expressed with respect to the ground state of ^{4}He. Column 3 lists the results obtained by Cohen and Kurath. The bracketed value is obtained from the Sussex interaction with $\epsilon_{p1/2} = 5.03$ MeV and $\epsilon_{p3/2} = 1.63$ MeV.

Nucleus	Binding energy (MeV)		
	Present	CK	Expt.
^{7}Li	13.57	13.67	11.95
	(12.13)		
^{9}Be	31.91	31.98	32.50
^{11}B	52.23	52.42	52.52
^{13}C	74.72	75.24	76.05

that the agreement between the resulting spectra of the present work and those of SM-I and SM-II is good as far as the low-lying normal parity states are concerned. This is confirmed in a number of cases by computing other observables,
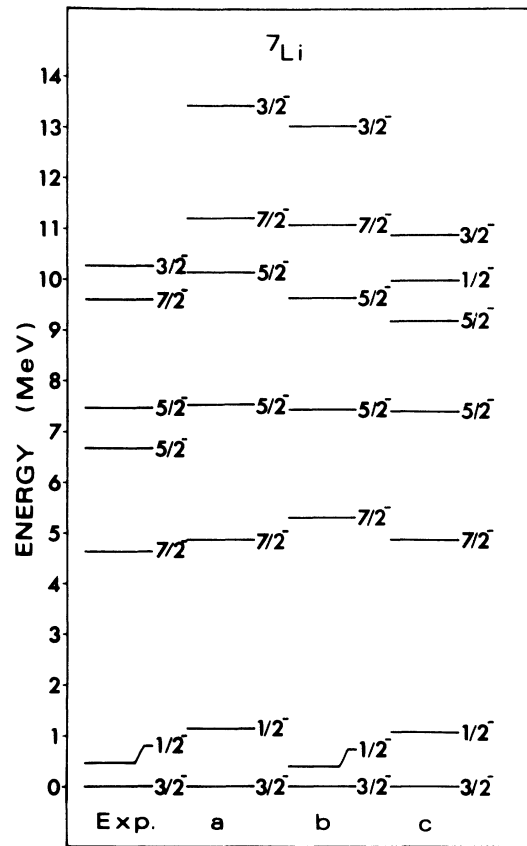

FIG. 1. The level scheme of ^{7}Li with levels identified by J^π. All levels have $T = \frac{1}{2}$. Column 1 is experimental and column 2 (a) results from the projected Hartree-Fock method (PHF) using the (6−16) 2BME interaction of Ref. 8. Column 3 (b) results from the PHF using the Sussex realistic interaction, and column 4 (c) is the shell-model spectra of SM-I.
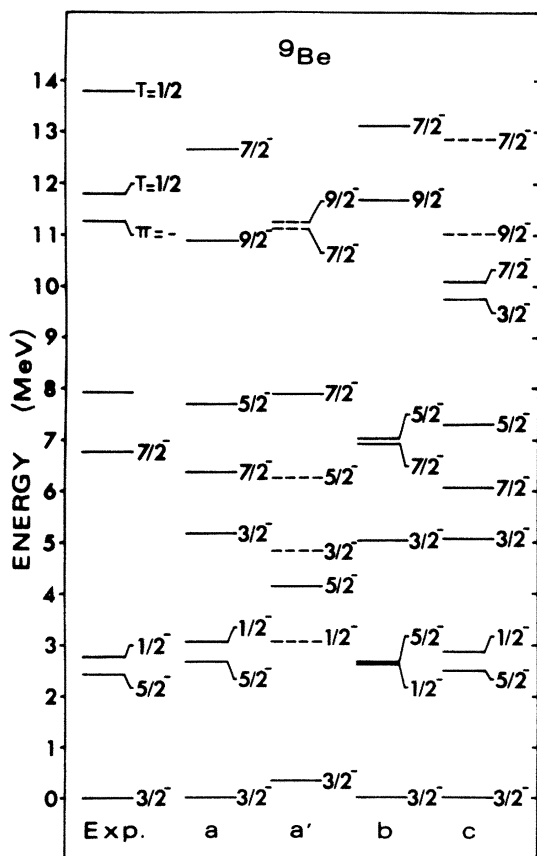
FIG. 2. The level scheme of ^{9}Be. See caption of Fig. 1 for columns 1 and 2. The intrinsic bands before mixing are shown in column 3 (a'), and column 4 (b) results from the PHF mixing using the Sussex realistic interaction. Column 5 (c) is the shell-model spectrum of SM-I obtained from the (6–16) 2BME interaction of Ref. 8, except the levels with dashed lines which result from the (8–16) 2BME interaction of the same reference.

FIG. 3. The level scheme of ^{11}B. See caption of Fig. 2 for details.

as will be seen in the following sections. It is worthwhile to stress the band-mixing character in the present calculation. Thus, the spectra of ^{9}Be and ^{11}B are not generated directly from a unique projection, as is done generally in other projected HF formalisms, but from mixed of two intrinsic HF orbitals after projection.

1. ^{7}Li

The intrinsic orbitals set up for ^{7}Li are of the form

$$\alpha^\dagger_{nk}\alpha^\dagger_{n-k}\alpha^\dagger_{pk}|^4\text{He}\rangle, \tag{13}$$

where n and p refer to neutrons and protons and k is equal to $\frac{1}{2}$ or $\frac{3}{2}$. In fact, we have used the corresponding conjugate orbital referenced to the
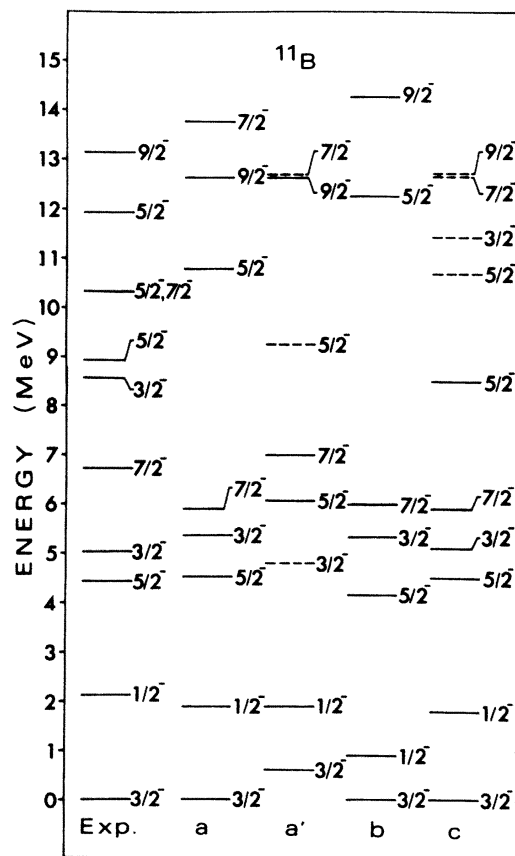
^{16}O core. As is seen in Fig. 1, the resulting spectra have a strong resemblance to the shell-model calculation of SM-I. In particular, the shell-model binding energy of the ground state of ^{7}Li in the field of ^{4}He differs by 1.72 MeV from the experimental value in SM-I and this feature is also observed in the present calculation. The shell-model calculation of SM-II removes this shortcoming and the difficulty of making the first $\frac{1}{2}^-$ state as low as at 0.48 MeV. The spectra in column (b) of Fig. 1, obtained by using the Sussex effective interaction in the present method, are also quite similar to those of the shell-model prediction of SM-II using the same force. The second $\frac{7}{2}^-$ state at 11.07 MeV, predicted both by SM-II and the present work, may correspond to the energy level at 9.61 MeV. The Sussex effective interaction has a tendency towards raising the states, except for the first two excited states, as is seen in column (b) of Fig. 1. This feature can also be observed in the spectra of SM-II which uses the same interaction.
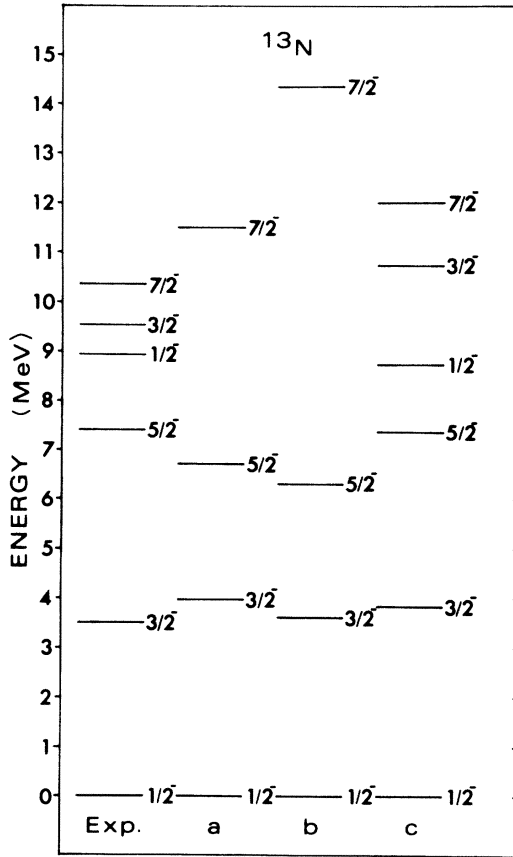
FIG. 4. The level scheme of ^{13}N. See caption of Fig. 1 for details.

2. ^9Be

The low-lying normal parity states can be generated from the prolate deformed HF solutions. The corresponding intrinsic orbitals are

$$\alpha_{nk_1}\alpha_{n-k_1}\alpha_{pk_1}\alpha_{p-k_1}\alpha_{pk_2}\alpha_{p-k_2}\alpha_{n-k_2}\left|^{16}O\right\rangle , \tag{14}$$

with k_1 and k_2 equal to $\frac{1}{2}$ or $\frac{3}{2}$. These two intrinsic orbitals are mixed after angular momentum projection, and the calculated spectra are similar to the shell-model calculations of SM-I and SM-II.

The spectra of this nucleus and those of $A = 11$ nuclei are the only instances known which can be treated within the framework of the rotational band mixing. The columns (a') and (a) of Fig. 2 show respectively the spectra before and after mixing. We see three sets of inversions due to the mixing; between the $\frac{1}{2}^-$ and first $\frac{3}{2}^-$ states, the second $\frac{5}{2}^-$ and first $\frac{7}{2}^-$ states, and finally the second $\frac{7}{2}^-$ and first $\frac{9}{2}^-$ states. The third $\frac{3}{2}^-$ state, predicted at 9.78 MeV by SM-I, is absent in the present study because of the limited configuration space in which

we solve the problem. The $\frac{9}{2}^-$ state of 10.91 MeV of the present calculation corresponds to the same spin state at 11.026 MeV of SM-I, shown in column (c) of Fig. 2, which results from the (8–16) two-body matrix elements (2BME) interaction of SM-I. Similarly, our second $\frac{7}{2}^-$ state may be compared with the third $\frac{7}{2}^-$ state of SM-I, also shown in column (c) of Fig. 2.

When the Sussex effective interaction is applied with the energy-splitting $\epsilon_{p1/2} - \epsilon_{p3/2} = 5.4$ MeV, which corresponds to the energy splitting of 2.8 MeV with respect to the ^{4}He core, the resulting spectrum shown in column (b) of Fig. 2 is very similar to the shell-model calculation of SM-II. Thus the first two excited states, which are very near each other, are in reverse order in comparison with the spectrum obtained from the two-body interaction of SM-I. It is noted that the shell-model calculation of Halbert, Kim, and Kuo[10] using the Hamada-Johnston potential was not able to reproduce correctly the first $\frac{1}{2}^-$ state. According to the projected HF calculation of Bouten et al.,[7] based on the LS coupling, using one-body spin-orbit forces in addition to the two-body interaction of Brink, the spin-orbit strength has to be raised up to the order of 3 MeV or more in order to reproduce the $\frac{1}{2}^-$ state higher than the $\frac{3}{2}^-$ state. However, in this calculation, the $\frac{7}{2}^-$ state is always higher than the second $\frac{5}{2}^-$ state whatever the variation of the spin-orbit strength may be.

3. ^{11}B

Contrary to the $A = 7$ and 9 mass nuclei discussed in the previous sections, this nucleus is characterized by the oblate deformed solutions of the Hartree-Fock equation. The intrinsic orbitals are written as

$$\alpha_{n1/2}\alpha_{n-1/2}\alpha_{p1/2}\alpha_{p-1/2}\alpha_{p-k}\left|^{16}O\right\rangle , \tag{15}$$

with k having $\frac{1}{2}$ or $\frac{3}{2}$. The columns (a') and (a) of Fig. 3 show respectively the resulting spectra before and after mixing of the two projected states. As in the case of ^{9}Be, the right level sequence is possible only after mixing. Thus, the order of the second $\frac{3}{2}^-$ and first $\frac{5}{2}^-$ states is reversed and the positions of the other states are much changed after diagonalization of the nuclear Hamiltonian within the orthonormalized basis. The correction made in the structure of the ground state wave function by mixing of two bands also influences the binding energy, the static moment, and the electromagnetic transition rates. An interesting feature is the change of the second $\frac{3}{2}^-$ state from 9.27 MeV before mixing to 10.81 MeV after diagonalization. The shell-model calculation of SM-II predicts the second $\frac{5}{2}^-$ state at about the

same energy as in the present work, and the results of SM-II in this energy region are much different from those obtained by SM-I. Again, use of the Sussex effective interaction in the projected HF method yields the spectra, shown in column (b) of Fig. 3, which are very similar to the shell-model calculation using the same interaction force. It is interesting to note that the strong rotation-particle coupling (RPC) model applied by Cavaignac, Jang, and Worledge,[1] yields a remarkable fit up to the first $\frac{7}{2}^-$ state, showing in some sense a validity of the RPC model for this nucleus. However, the rotational parameters used by these authors, such as the RPC strength, the moment of inertia, the decoupling factor, and the initial energy separation of two $J = \frac{3}{2}$ states before mixing, were obtained by fitting the energies of the lowest five levels. The lack of physical support for these parameters has a consequence for the magnetic moment, as well as for the $M1$ transition rates, which are in disagreement with the observed values.[14] The recently confirmed $\frac{3}{2}^-$ state at 8.57 MeV has not been reproduced by any shell-model calculation and this still remains as an unsolved question. The position of the $\frac{9}{2}^-$ state at 12.62 MeV can be compared with that predicted by SM-I at 12.73 MeV resulting from the (8–16) 2BME interaction of Ref. 8.

4. ^{13}N

From the point of rotational model, the first four low-lying levels are those belonging to the ground state band which terminates at the $\frac{7}{2}^-$ state. The intrinsic orbital for this band is written as

$$\alpha_{nk}\alpha_{n-k}\alpha_{p-k}\,|^{16}O\rangle, \qquad (16)$$

with $k = \frac{1}{2}$. It is known that the ground state of ^{13}N is well represented by a relatively pure (90%) $1p_{1/2}$ single-particle state. This is confirmed by the HF solution for the orbital under consideration.

As is seen in Fig. 4, the three negative parity states just above the $\frac{7}{2}^-$ state cannot be obtained from the model presented, due to the limited configuration space assumed. It is expected that the assumption of pure $1p$ configurations is less valid near the ^{16}O nucleus.

It is interesting to note the large energy difference between the $\frac{7}{2}^-$ state at 11.51 MeV in column (a) of Fig. 4 and the same spin state at 14.35 MeV in column (b) of the same figure. Such an energy difference is also observed between the two shell-model calculations previously cited. Thus SM-I predicts the $\frac{7}{2}^-$ state at about 12 MeV, whereas SM-II with the Sussex interaction obtains the state at 15.2 MeV.

B. Magnetic moments and $M1$ transitions

The resulting wave functions are tested by calculating magnetic dipole moments and $M1$ transition rates. For $1p$-shell nuclei, there is some concrete information[15] concerning the usefulness of the unperturbed $M1$ operator. Magnetic moments and $B(M1)$ strengths calculated for a variety of $(1s)^4(1p)^{A-4}$ shell model have been shown to be in fairly good agreement with measured quantities. Therefore, the configuration-excitation corrections to the $M1$ operator, which are estimated in second-order perturbation, are expected to be very small. Accordingly, the evaluation of magnetic dipole moments and $M1$ transition has been carried out assigning the free-nucleon magnetic moments to all the nucleons.

The calculated magnetic dipole moments for the ground states of $A = 7$, 9, 11, and 13 mass nuclei are shown in Table III and are compared with those[16] obtained from the shell-model calculation of SM-I. The agreement between two results is fairly good. As in the case of binding energies, inadequate choice of the intrinsic HF orbitals leads to inconsistent magnetic dipole moments. For example, the oblate deformed solution yields $0.22\,\mu_N$ for the magnetic dipole moment of the ^9Be ground state, whereas the prolate deformed solution is able to reproduce the correct sign and gives $-1.298\,\mu_N$. The value calculated in the present work is quite similar to that of SM-I, $-1.297\,\mu_N$. In the case of ^7Li, however, two intrinsic orbitals, one with $k = \frac{1}{2}$ particles and other filled with $k = \frac{3}{2}$ particles out of the ^4He core, yield almost the same magnetic dipole moments $3.199\,\mu_N$ and $3.032\,\mu_N$, respectively, for the $J = \frac{3}{2}$ states.

Table IV shows the theoretical $M1$ transition strengths which are compared with the strengths determined from the results of SM-I. There is a good overall agreement between the present approach and the shell-model calculation.

We should comment on the transition between the $\frac{5}{2}^-$ and ground states of ^7Li. All shell-model

TABLE III. Magnetic dipole moments (nuclear magnetons) for the ground states identified in columns 1 and 2. Column 4 lists the results obtained by Cohen and Kurath.

Nucleus	J^π	Magnetic moment (μ_N)		
		Present	CK	Expt.
^7Li	$\frac{3}{2}^-$	3.199	3.170	3.256
^9Be	$\frac{3}{2}^-$	−1.298	−1.297	−1.177
^{11}B	$\frac{3}{2}^-$	2.617	2.505	2.688
^{13}C	$\frac{1}{2}^-$	0.708	0.701	0.702
^{13}N	$\frac{1}{2}^-$	0.332		0.322

TABLE IV. Magnetic dipole transition rates between normal parity states in odd-A nuclei. The states are identified by the quantum numbers $2J$, $2T$, and their excitation energies, except those followed by the letters Th, which have not yet been observed. Column 5 lists the $B(M1)$ values obtained by Cohen and Kurath.

Nucleus	Initial state $2J,2T$ [Ex (MeV)]	Final state $2J,2T$ [Ex (MeV)]	$B(M1)(\mu_N^2)$ Present	CK	Expt.
^{7}Li	1,1 [0.48]	3,1 [0.00]	4.46	4.44	4.75 ± 0.24
	5,1 [6.68]		0.0026	0.000 64	0.42
	5,1 [7.47]		0.078	0.039	0.184 ± 0.082
^{9}Be	5,1 [2.42]	3,1 [0.00]	0.39	0.40	0.745 ± 0.096
	1,1 [2.78]		2.53	2.35	
	3,1 [5.17] Th		0.31	0.33	
	7,1 [6.76]	5,1 [2.43]	0.28	0.39	
	3,1 [5.17] Th		1.88	1.84	
^{11}B	1,1 [2.12]	3,1 [0.00]	1.69	1.80	1.198 ± 0.067
	5,1 [4.44]		0.52	0.52	0.56 ± 0.25
	3,1 [5.02]		1.42	1.35	1.16 ± 0.23
	5,1 [8.93]		0.026	0.38	0.525 ± 0.070
	3,1 [5.02]	1,1 [2.12]	1.04	0.99	0.56 ± 0.11
	3,1 [5.02]	5,1 [4.44]	3.05	2.79	
	7,1 [6.74]		0.013	0.012	
^{13}C	3,1 [3.68]	1,1 [0.00]	0.94	1.19	0.763 ± 0.070
	5,1 [7.55]	3,1 [3.68]	0.013	0.0047	
^{13}N	3,1 [3.51]	1,1 [0.00]	1.31	1.62	1.32
	5,1 [7.39]	3,1 [3.51]	0.0084	0.0038	

probabilities are quite small when comparison is made with the old empirical data[16] determined from the peak cross sections of the inverse radiative capture reaction of ^{3}H on ^{4}He. The present calculation has also a strong resemblance to the shell-model calculations. However, a marked exception to the overall agreement occurs for the second $\frac{5}{2}^-$ state of ^{11}B. The $M1$ transition strength between this state and the ground state is much smaller than the predicted strength of SM-I. As a consequence, the state in question at 10.81 MeV may correspond to the level predicted at 10.69 MeV by the shell-model calculation.

In contrast to the $M1$ operator, the $E2$ operator is very sensitive to admixtures of other configurations. Therefore, calculation of electric quadrupole moments and $E2$ transition rates in the present model may not be of much significance.

C. Moments of inertia

A method for computing microscopically the moment of inertia is the Inglis cranking formula[17,4] given by

$$\mathcal{J} = 2 \sum_{\sigma,\mu} \frac{|\langle \sigma | J_x | \mu \rangle|^2}{E_\sigma - E_\mu}, \tag{17}$$

where σ refers to an unoccupied orbital and μ to an occupied orbital. The energies in the denominator are the eigenvalues of the HF Hamiltonian. Inasmuch as the gap between the filled and empty

orbits has little effect on spectra obtained from HF projection, the cranking formula can be used.

The resulting moment of inertia parameters $\hbar^2/(2\mathcal{J})$ of $A = 6$, 8, 10, and 12 nuclei are shown in Fig. 5, where the values for both the oblate and prolate deformed solutions are given. The reason for computing the moments of inertia only for the even mass nuclei resides in the fact that the intrinsic orbitals corresponding to the ground state are pure and are completely filled or half filled. This is not the case for the odd-mass nuclei, as was seen in the preceding discussion. It should be noted that the energy gap between the filled and empty orbits of $A = 8$ is 1.2 MeV in the oblate deformed HF solution, whereas the gap in the prolate deformed solution extends to about 11.7 MeV. Kurath and Pičman[2] have estimated that the moment of inertia of ^{11}B may be near 1 MeV, deduced from the argument that the ratio of the spin-orbit coupling strength to the inverse moment of inertia lies between 8 and 1, and is something like 4. Cavaignac et al.[1] have used the value of 0.892 MeV in the RPC model calculation for ^{11}B. This value is very close to the estimated moment of inertia parameter from Fig. 5. The rotational band structure studies based on the simple Nilsson model predict 0.486 and 0.54 MeV, respectively, for the moment of inertia parameters of ^{9}Be and ^{7}Li. These values are somewhat smaller than those corresponding to the prolate deformed orbital in Fig. 5. It is interesting to compare the two
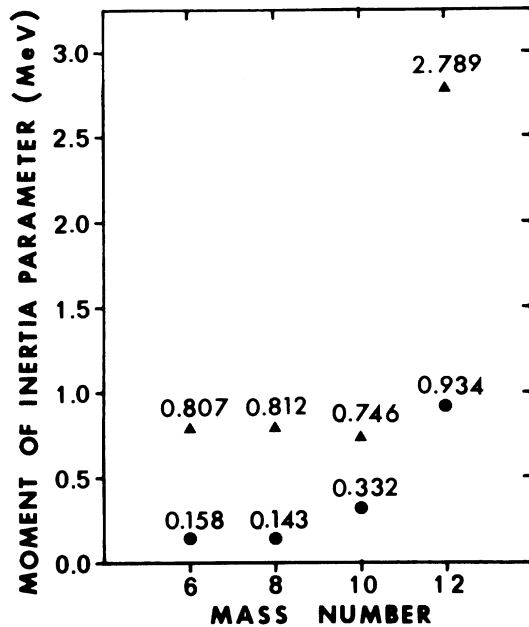
FIG. 5. The moment of inertia parameters for the ground states of $A = 6$, 8, 10, and 12 nuclei, obtained by using the cranking formula. The triangles are from the prolate solutions and the darkened circles are from the oblate solutions.

moments of inertia of ^{12}C, corresponding to two different kinds of deformation. The value of 2.79 MeV obtained from the prolate deformation is larger than the physically expected moment of inertia. This is because the energy gap in the prolate solution is 5.7 MeV as against 12.3 MeV obtained in the oblate solution, and this gap has a considerable effect on the spectra of ^{12}C. Therefore, the applicability of the cranking model to the prolate HF solution of ^{12}C is less evident and the oblate deformation is favored. Kelson and Levinson[4] have shown in their study of the sd-shell nuclei that the cranking model agrees well with the Skyrme formula,[18] the accuracy of which is expected to be good because it is based on a variational principle. We have not attempted to apply this alternative method for computing the moment of inertia.

IV. CONCLUSIONS

In this work, we have attempted to see how good an approximation to the complete diagonalization one gets for the odd-even mass nuclei with the mixing of a few Hartree-Fock projected orbitals. In particular, we have investigated in a self-consistent way the nuclear collective properties of odd-mass nuclei of the $1p$ shell. The overall agreement between the present calculations and shell-model calculations for the spectra and the

results for the magnetic moments, as well as on $M1$ transitions, have been shown to be a good test of the wave functions resulting from the self-consistent axially deformed orbitals. Although the spectra of the present study resemble those obtained from the strong coupling rotational model based on the simple Nilsson's deformed potential, the very large energy gap between occupied and empty orbits in the HF solutions makes an essential difference from the macroscopic approach. Moreover, in contrast to the phenomenological band-mixing calculation, the present method does not employ the rotation-particle coupling interaction.

As was mentioned in the introduction, there is clearly a limit as to how far one can proceed using the present approach. The assumption of pure $1p$-shell configurations obliges us to compute the single-particle levels in a restricted self-consistent way. Also, because of the limited configuration space, the resulting spectra sometimes suffer a loss of certain high-lying states, especially in the case of ^{13}N. Nevertheless, it is concluded that the much smaller basis used in the present work allows us to describe adequately the main collective features of the low-lying state of odd-A $1p$-shell nuclei.

The authors wish to thank Dr. A. J. Cole and Dr. R. Piepenbring for helpful discussions and for carefully reading the manuscript.

APPENDIX: EFFECT OF THE CENTER OF MASS CORRECTION

The effect of the center of mass (c.m.) correction on the HF calculations can be investigated by computing the HF energy E_{HF}, the mass quadrupole moment Q_0, and the mean square radius r_m^2 from the HF solutions obtained with and without subtraction of the energy of the c.m. motion of the whole system from the total Hamiltonian. We take an axially symmetric ground state configuration of $A = 9$ mass nucleus as an example. The single-particle HF wave functions are expanded in terms of the oscillator states of the $N = 0$, 1, and 2 major shells using the effective force No. 1 of Volkov.[7] The resulting HF energy, rms radius, and mass quadrupole moment are $E_{HF} = -44.11$ (-29.89) MeV, $r_m = 2.30$ (2.29) fm, and $Q_0 = 33.11$ (34.11) fm^2, where the bracketed values are obtained without correction of the c.m. motion. Thus, only the HF energy changes appreciably and such a change would certainly be observed in the HF calculation of other $1p$-shell nuclei.[19] For the ground state HF problem, the c.m. motion can be assumed to be in the $1s$-shell state and thus the kinetic energy of the c.m. motion amounts to $3/4\hbar\omega$. This quantity is significant when compared with the total kinetic

energy of the system in $1p$-shell nuclei, 100–200 MeV, from which the kinetic energy of the c.m. motion is subtracted. However, the effect of the c.m. correction on the HF wave functions is insignificant, as is seen from the values of the rms radius and mass quadrupole moment. Therefore, inasmuch as the spectroscopic calculations using the projected states from the HF wave functions are concerned, we can safely use the HF wave functions obtained without the c.m. correction.

[1]A. B. Clegg, Phil. Mag. 6, 1207 (1961); Nucl. Phys. 38, 353 (1962); C. M. Chesterfield and B. M. Spicer, Nucl. Phys. 41, 675 (1963); F. El-Batanoni and A. A. Kresnin, Nucl. Phys. 89, 577 (1966); A. C. Slight, T. E. Drake, and G. R. Bishop, Nucl. Phys. A208, 157 (1973); J. C. Cavaignac, S. Jang, and D. H. Worledge, Nucl. Phys. A243, 349 (1975).

[2]D. Kurath and L. Pičman, Nucl. Phys. 10, 313 (1959).

[3]A good summary together with related references of the subject is given by G. Ripka, in *Advances in Nuclear Physics*, edited by M. Baranger and E. Vogt (Plenum, New York, 1968), Vol. 1, p. 183.

[4]I. Kelson, Phys. Rev. 132, 2189 (1963); I. Kelson and C. A. Levinson, Phys. Rev. 134, B269 (1964).

[5]By the projected HF calculations we understand either projection before or after the variational calculation.

[6]W. H. Bassichis, B. Giraud, and G. Ripka, Phys. Rev. Lett. 15, 930 (1965).

[7]See, for example, for p-shell nuclei, A. B. Volkov, Nucl. Phys. 74, 33 (1965); M. Bouten, M.-C. Bouten, H. Depuydt, and L. Schotsmans, *ibid.* A127, 177 (1969); M. R. Gunye, J. Law, and R. K. Bhaduri, *ibid.* A132, 225 (1969).

[8]S. Cohen and D. Kurath, Nucl. Phys. 73, 1 (1965); A101, 1 (1967).

[9]P. S. Hauge and S. Maripuu, Phys. Rev. C 8, 1609 (1973).

[10]D. Amit and A. Katz, Nucl. Phys. 58, 388 (1964); M. H. Hull, Jr., and C. Shakin, Phys. Lett. 19, 506 (1965); E. C. Halbert, Y. E. Kim, and T. T. S. Kuo, *ibid.* 20, 657 (1966); R. L. Becker and A. D. Mackellar, *ibid.* 21, 201 (1966); S. Varmo and P. Goldhammer, Nucl. Phys. A125, 193 (1969).

[11]See, for example, Ref. 3 and also K. T. R. Davies, S. J. Krieger, and M. Baranger, Nucl. Phys. 84, 545 (1966).

[12]I. Unna, Phys. Rev. 132, 2225 (1963).

[13]A. K. Kerman, K. Dan. Vidensk. Selsk. Mat.–Fys. Medd. 30, No. 15 (1956).

[14]J. F. Cavaignac (private communication).

[15]E. C. Halbert, J. B. McGrory, B. H. Wildenthal, and S. P. Pandya, in *Advances in Nuclear Physics*, edited by M. Baranger and E. Vogt (Plenum, New York, 1971), Vol. 4, p. 315.

[16]Because the shell-model calculations of Refs. 8 and 9 are compared with the experimental results, these empirical values are also cited in Tables II, III, and IV.

[17]D. R. Inglis, Phys. Rev. 96, 1059 (1954).

[18]T. H. R. Skyrme, Proc. Phys. Soc. (London) A70, 433 (1957); C. A. Levinson, Phys. Rev. 132, 2184 (1963).

[19]The c.m. correction to the HF energy in the $2s$-$1d$ shell is almost negligible. See, for example, M. R. Gunye, Nucl. Phys. A118, 174 (1968).